

Level Set Methods for Fluid Interfaces

J.A. Sethian and Peter Smereka***

*Dept. of Mathematics, University of California, Berkeley, California

**Dept. of Mathematics, University of Michigan, Ann Arbor, Michigan

ABSTRACT:

We provide an overview of level set methods, introduced by Osher and Sethian, for computing the solution to fluid interface problems. These are computational techniques which rely on an implicit formulation of the interface, represented through a time-dependent initial value partial differential equation. We discuss the essential ideas behind the techniques, the coupling of these techniques to finite difference methods for incompressible and compressible flow, and a collection of applications including two phase flow, ship hydrodynamics, and inkjet printhead design.

CONTENTS

INTRODUCTION AND OVERVIEW	2
REPRESENTATION AND TRACKING OF MOVING INTERFACES	3
LEVEL SET ALGORITHMS FOR MOVING INTERFACES	5
<i>Propagating Curves and Hyperbolic Conservation Laws</i>	5
<i>Level Set Methods</i>	6
NUMERICAL ISSUES: EFFICIENCY, ADAPTIVITY, AND ACCURACY	8
<i>Limiting Computational Labor; The Narrow Band Approach</i>	8

<i>Construction of Extension Velocities</i>	8
<i>Initialization, Reinitialization, and Solving for Extension Velocities</i>	9
<i>Additional Numerical Comments and Recent Developments</i>	11
<i>Advantages and Disadvantages of Level Sets</i>	11
TWO-PHASE FLOWS	13
<i>Density Weighted Divergence-Free Projection</i>	14
<i>Level Set Formulation</i>	14
<i>Thick Interfaces</i>	14
<i>Numerical Issues</i>	15
<i>Recent Developments</i>	17
<i>Compressible Two-Phase Flows</i>	18
<i>Example Application: The Design of Inkjet Printheads</i>	20
PROBLEMS IN MATERIAL SCIENCE	22
<i>Example Application: Faceted Polycrystalline Thin Films</i>	22
CONCLUSIONS	24

1 INTRODUCTION AND OVERVIEW

A large collection of fluid problems involve moving interfaces. Applications include air-water dynamics, breaking surface waves, solidification melt dynamics, and combustion and reacting flows. In many such applications, the interplay between the interface dynamics and the surrounding fluid motion is subtle, with factors such as density ratios and temperature jumps across the interface, surface tension effects, topological connectivity and boundary conditions playing significant roles in the dynamics.

Over the past fifteen years, a class of numerical techniques known as level set methods have been built to tackle some of the most complex problems in fluid interface motion. Level set methods, introduced by Osher and Sethian, are computational techniques for tracking moving interfaces; they rely on an implicit representation of the interface whose equation of motion is numerically approximated using schemes built from those for hyperbolic conservation laws. The resulting techniques are able to handle problems in which the speed of the evolving interface may sensitively depend on local properties such as curvature and normal direction, as well as complex physics off the front and internal jump

and boundary conditions determined by the interface location. Level set methods are particularly designed for problems in multiple space dimensions in which the topology of the evolving interface changes during the course of events, and problems in which sharp corners and cusps are present.

In this review, we discuss the numerical development of these techniques and their application to a collection of problems in fluid mechanics, including incompressible and compressible flow, and applications to bubble dynamics, ship hydrodynamics, and inkjet printhead design. We note that there already exists a collection of review articles and books on these techniques, and refer the interested reader to works by Osher & Fedkiw (2001) and Sethian (1996b 1996c, 1999a, 1999b, 2001).

2 REPRESENTATION AND TRACKING OF MOVING INTERFACES

There are at least three ways to characterize moving interfaces. For ease of exposition, we consider the case of a closed curve moving in the plane. More precisely, consider a simple closed curve $\Gamma(t)$ moving in two dimensions. Assume that a given velocity field $\vec{u} = (u, v)$ transports the interface. All three constructions carry over to three dimensions. Here, we follow closely the discussion in Sethian (2001).

- **The Geometric View:** Suppose one parameterizes the interface, that is, $\Gamma(t) = (x(s, t), y(s, t))$. Then one can write (see, for example, Sethian 1999) the equations of motion in terms of individual components $\vec{x} = (x, y)$ as

$$\begin{aligned} x_t &= u \frac{y_s}{(x_s^2 + y_s^2)^{1/2}}, \\ y_t &= -v \frac{x_s}{(x_s^2 + y_s^2)^{1/2}}. \end{aligned} \tag{1}$$

This is a differential geometry view; the underlying fixed coordinate system has been abandoned, and the motion is characterized by differentiating with respect to the parameterization variable s .

- **The Set Theoretic View:** Consider the characteristic function $\chi(x, y, t)$, where χ is one inside the interface Γ and zero otherwise. Then one can write the motion of the characteristic function as

$$\chi_t = -\mathbf{u} \cdot \nabla \chi \tag{2}$$

In this view, all the points inside the set (that is, where the characteristic function is unity) are transported under the velocity field.

- **The Analysis View:** Consider the function $\phi : R^2 \times [0, \infty) \rightarrow R$, defined so that the zero level set $\phi = 0$ corresponds to the evolving front $\Gamma(t)$. In this way the front is implicitly defined. Then the equation for the evolution

of ϕ corresponding to the motion of the interface is given by

$$\phi_t + \mathbf{u} \cdot \nabla \phi = 0 \tag{3}$$

Each view has resulted in its own numerical methodology. The first leads to marker particle and string methods which discretize the underlying coordinate-free differential geometry view; this is a moving, Lagrangian representation. The second, characteristic function view leads to volume-of-fluid methods, which discretize the underlying domain and fill cell fractions with values that represent the characteristic function in those cells; these values are zero or one except in those cells cut by the interface. The third, implicit view, approximates the above time-dependent partial differential equation through a discretization of the evolution operators on a fixed grid.

We note that each approach has its virtues and drawbacks. Nonetheless, in this review article we shall focus on the third category. Here, the associated numerical techniques known as level set methods (Osher & Sethian 1988) approximate the solution of this time-dependent initial value problem to follow the evolution of the associated level set function whose zero level set always gives the location of the propagating interface.

In order to take this implicit approach, several issues must be confronted. First, we need to devise an appropriate theory and strategy for choosing the correct weak solution once smoothness in the front is lost; this is, in part, built on the work of Crandall and Lions (1983, 1984) on viscosity solutions of Hamilton-Jacobi equations and some work on front propagation and its link with hyperbolic conservation laws developed by Sethian (1982, 1985, 1987). It is not *a priori* clear that the viscosity solution is the correct solution for a given physical problem but nevertheless this assumption is built into level set methods.

Second, the Osher-Sethian level set technique which discretizes the above requires an additional space dimension to carry the embedding, and hence is computationally inefficient for many problems. This is rectified through the adaptive Narrow Band Method given by Adalsteinsson & Sethian (1995a) and Peng et al (1999a), which will be discussed below.

Third, since both the level set function and the velocity field defined at the interface are defined throughout all of space, one must devise appropriate extension velocities to transport the neighboring level set functions in tandem with the one corresponding to the zero level set. Techniques for doing so were introduced by Malladi et al (1995) Zhao et al (1996), Chen et al (1997) and Adalsteinsson & Sethian (1999). These will be discussed below.

3 LEVEL SET ALGORITHMS FOR MOVING INTERFACES

3.1 Propagating Curves and Hyperbolic Conservation Laws

3.1.1 Viscosity Solutions and Entropy Conditions

Consider the simple case of a periodic curve propagating in the plane in a direction normal to itself with speed F . We follow the discussion in Sethian (1987) and analyze this problem in some detail. Consider the initial front given by the graph of $f(x)$, with f and f' periodic on $[0, 1]$, and suppose that the propagating front remains a graph for all time. Let ψ be the height of the propagating function at time t , and thus $\psi(x, 0) = f(x)$. The tangent at (x, ψ) is $(1, \psi_x)$. The change in height V in a unit time is related to the speed F in the normal direction by

$$\frac{V}{F} = \frac{(1 + \psi_x^2)^{1/2}}{1}, \quad (4)$$

and thus the equation of motion becomes

$$\psi_t = F(1 + \psi_x^2)^{1/2}. \quad (5)$$

Let us consider two cases in some detail. First, suppose that the speed function F is constant (set equal to unity for simplicity). This means that the propagating front at time t corresponds to the set of all points located a distance t from the initial front. It is easy to see that this not a differentiable function (see Figure 1a). Consequently, we need a definition of a weak solution which has meaning beyond the point where differentiability is lost. One way is through the construction suggested in Sethian (1982): “if the front is viewed as a propagating flame front, then once a particle is burnt it remains burnt”. This is an appropriate view if one considers the front as a boundary separating two physical regimes.

Now, consider the case of a speed function F which depends on the local curvature, namely $F = 1 - \epsilon\kappa$. The effects of curvature act as a mitigating factor, and enforces a smooth solution to the problem. Use of the speed function $F(\kappa) = 1 - \epsilon\kappa$ and the formula $\kappa = -\psi_{xx}/(1 + \psi_x^2)^{3/2}$ yields

$$\psi_t - (1 + \psi_x^2)^{1/2} = \epsilon \frac{\psi_{xx}}{1 + \psi_x^2}. \quad (6)$$

The solution to the same initial value problem with this curvature-driven speed function is shown in Figure 1b; one can see that the solution remains smooth.

From a theoretical point of view, it can be shown that the limit as the curvature term goes to zero of the smooth solutions is in fact the entropy-satisfying weak solution shown above. The constant speed front propagation initial value partial differential equation given above is a special case of a Hamilton-Jacobi equation, and the general theory of viscosity solutions developed by Crandall & Lions (1983, 1984) shows that limiting case of a Hamilton-Jacobi equation with smoothing right-hand-side is the constant speed entropy case.

3.1.2 Links with Hyperbolic Conservation Laws

We now differentiate both sides of Eqn. 5, to produce an evolution equation for the slope $u = d\psi/dx$ of the propagating front, namely,

$$u_t + [-(1 + u^2)^{1/2}]_x = \epsilon \left[\frac{u_x}{1 + u^2} \right]_x. \quad (7)$$

Thus, following Sethian (1987), the derivative of the curvature-modified equation for the changing height ψ looks like some form of a viscous hyperbolic conservation law, with $G(u) = -(1 + u^2)^{1/2}$ for the propagating slope u . Hyperbolic conservation laws of this form have been studied in considerable detail and the entropy condition (Sethian 1982) is equivalent to the one for propagating shocks in hyperbolic conservation laws.

Given this connection, the next step in development of PDE-based interface advancement techniques was to in fact exploit the considerable numerical technology for hyperbolic conservation laws to tackle front propagation itself, as suggested by Sethian (1987). In such problems, schemes are specifically designed to construct entropy-satisfying limiting solutions and maintain sharp discontinuities wherever possible; these goals are required to keep fluid variables such as pressure from oscillating, and to make sure that discontinuities are not smeared out. This is equally important in the tracking of interfaces, in which one wants corners to remain sharp and to accurately track intricate development.

3.2 Level Set Methods

3.2.1 Formulation

The above discussion focussed on curves which remain graphs. Two pivotal aspects of the Osher-Sethian (1988) approach are the embedding of the interface in a higher dimensional function, allowing the implicit framework to embrace problems which do not remain graphs and which can change topology, and the development of multi-dimensional upwind schemes to approximate the relevant gradients. Here, we follow with little change the discussion given by Sethian (2001).

Level set methods rely on two central embeddings; first the embedding of the interface as the zero level set of a higher dimensional function, and second, the embedding (or extension) of the interface's velocity to this higher dimensional level set function. More precisely, given a moving closed hypersurface $\Gamma(t)$, that is, $\Gamma(t = 0) : [0, \infty) \rightarrow R^N$, propagating with a speed F in its normal direction, we wish to produce an Eulerian formulation for the motion of the hypersurface propagating along its normal direction with speed F , where F can be a function of various arguments, including the curvature, normal direction, etc. Let $\pm d$ be the signed distance to the interface. If this propagating interface is embedded as the zero level set of a higher dimensional function ϕ , that is, let $\phi(x, t = 0)$, where $x \in R^N$ is defined by

$$\phi(x, t = 0) = \pm d, \quad (8)$$

then an initial value partial differential equation can be obtained for the evolution of ϕ , namely

$$\phi_t + F|\nabla\phi| = 0 \quad (9)$$

$$\phi(x, t = 0) \text{ given} \quad (10)$$

This is the level set implicit formulation of front propagation taken by Osher & Sethian (1988).

There are certain advantages associated with this perspective. First, it is unchanged in higher dimensions, that is, for surfaces propagating in three dimensions and higher. Second, topological changes in the evolving front Γ are handled naturally; the position of the front at time t is given by the zero level set $\phi(x, y, t) = 0$ of the evolving level set function. This set need not be connected, and can break and merge as t advances. Third, terms in the speed function F involving geometric quantities such as the normal vector \mathbf{n} and the curvature κ may be easily approximated through the use of derivative operators applied to the level set function, that is,

$$\mathbf{n} = \frac{\nabla\phi}{|\nabla\phi|} \quad \text{and} \quad \kappa = \nabla \cdot \frac{\nabla\phi}{|\nabla\phi|}.$$

Fourth, the upwind finite difference technology for hyperbolic conservation laws may be used to approximate the gradient operators.

3.2.2 Approximation Schemes

Entropy-satisfying upwind viscosity schemes for this initial value formulation were introduced by Osher & Sethian (1988). One of the simplest first order scheme for Eqn. 9 in two space dimension is given by:

$$\phi_{ij}^{n+1} = \phi_{ij}^n - \Delta t[\max(F_{ij}, 0)\nabla^+ + \min(F_{ij}, 0)\nabla^-], \quad (11)$$

where

$$\nabla^+ = \left[\begin{array}{c} \max(D_{ij}^{-x}, 0)^2 + \min(D_{ij}^{+x}, 0)^2 + \\ \max(D_{ij}^{-y}, 0)^2 + \min(D_{ij}^{+y}, 0)^2 \end{array} \right]^{1/2}$$

and

$$\nabla^- = \left[\begin{array}{c} \max(D_{ij}^{+x}, 0)^2 + \min(D_{ij}^{-x}, 0)^2 + \\ \max(D_{ij}^{+y}, 0)^2 + \min(D_{ij}^{-y}, 0)^2 \end{array} \right]^{1/2}$$

Higher order schemes are available, see Osher & Sethian (1988) and the schemes for non-convex flux laws developed by Osher & Shu (1991).

4 NUMERICAL ISSUES: EFFICIENCY, ADAPTIVITY, AND ACCURACY

4.1 Limiting Computational Labor; The Narrow Band Approach

The above implicit representation tracks *all* the level sets throughout the entire computational domain, even though interest is really confined only to the zero level set itself corresponding to the interface. We can estimate an operation count for this method as follows; assume a three-dimensional calculation, and thus with N grid points in each direction we have N^3 points in the mesh. To advance a front throughout the entire domain requires roughly N steps, leading to an $O(N^4)$ calculation. This clearly is wasteful, since it requires moving all the level sets, some very far from the region of interest.

Adalsteinsson & Sethian (1995a) introduced the idea of the “Narrow Band Approach”, which limits labor to a thin region around the zero level set itself. For example, in the above estimate, this means that the operation count is reduced to $O(N^3 * k)$ where k is the width of this narrow band. The savings are substantial; use of narrow band-type methods leads to tractable three-dimensional simulations. For details, see Adalsteinsson & Sethian (1995) and also Peng et al (1999a).

4.2 Construction of Extension Velocities

The implicit embedding inherent in the level set approach means that the velocity F that transports the interface must have meaning through the computational domain, not just on the front itself. Even with the use of the Narrow Band approach, one must be able to construct an *extension velocity* which advances the neighboring level sets, not just the zero level set.

How should one choose such an extension velocity? In some physical problems, such as those in fluid calculations, the velocity field may have a natural meaning away from the interface; in other simulations, such as those in materials sciences such as semiconductor profile evolution, the profile evolution law has no real meaning elsewhere, and a suitable extension must be devised.

As examples, Sethian and Strain (1992) developed a boundary integral formulation for dendritic solidification which they developed both on and off the front to provide an extension velocity. The two phase flow simulations of Sussman et al (1994) and Chang et al (1996) built extension velocities from the underlying fluid velocities; these are described in some detail below. In turbulent combustion calculations, Rhee et al (1995) built an extension velocity using an underlying elliptic partial differential equation coupled to a source term along the interface. In a different solidification approach, Chen et al (1997) worked directly with the partial differential equations and built an extension velocity by solving an advection equation in each component

The only real requirements for an extension velocity are that it be defined

away from the interface, and that it smoothly approach the prescribed interface velocity as the zero level set is approached. Malladi et al (1995) introduced the idea of building an extension velocity at each point in the domain by extracting the prescribed value at the closest point on the front. This idea can be used to obtain a general way of constructing extension velocities as follows. Suppose the extension velocity, which we call F_{ext} , satisfies the following:

$$\nabla F_{\text{ext}} \cdot \nabla \phi = 0. \quad (12)$$

It is straightforward (see Zhao et al 1996) to show that under this velocity field, the level set function ϕ remains the signed distance function for all time, assuming that both F and ϕ are smooth. Thus, at least theoretically, no bunching or stretching of neighboring level sets can occur. To solve Eqn. 12 there are three different approaches. The first such approach was suggested by Malladi et al (1995) in their work on shape segmentation; they find the closest point on the front, and extrapolate that velocity to the given grid point. This can be thought of as a method of characteristics solution to the underlying partial differential equations.

The second approach converts Eqn. 12 into the time dependent problem:

$$\frac{\partial F_{\text{ext}}}{\partial t} + \text{sign}(\phi) \frac{\nabla \phi}{|\nabla \phi|} \cdot \nabla F_{\text{ext}} = 0, \quad (13)$$

The above equation is a hyperbolic equation whose characteristics point outward from the interface in the normal direction. Thus as one solves Eqn. 13 information is carried from the interface into the rest of the domain. This idea was introduced by Chen et al (1997) and has been used and further developed by Zhao et al (1996) and Peng et al (1999a).

The third approach to solve Eqn. 12, introduced by Adalsteinsson & Sethian (1999), takes a two-tiered approach:

- First, given the level set function at time n , one produces a signed distance function $\bar{\phi}_{ij}^n$ around the zero level set (see below).
- Simultaneously, and in tandem, one solves the associated extension equation for F_{ext} satisfying Eqn. 12.

This is what is used to update the front. Finally, we note that in this construction, the signed distance function need not replace the one which represents the level set interface.

4.3 Initialization, Reinitialization, and Solving for Extension Velocities

In many situations it is preferable or necessary that the level set function be set to the signed distance function (see Eqn. 8). The reasons for this are threefold. First, narrow band methods and velocity extension constructions are more accurate when the signed distance function is used. Second, in applications where the interface is a given thickness, using a signed distance function for the level set function ensures that the interface has a fixed thickness. Third, using a signed

distance function indicates that the level set function will be well behaved near the interface.

It is not difficult to initialize the level set function to be the distance function, however, under the evolution of Eqn. 9 it will not necessarily remain so. Therefore at later times in the computation one must replace the level set function by a signed distance function without changing its zero level set. When this is performed at the beginning of the calculation, it is called initialization, when performed during the course of the calculation, it is referred to as reinitialization. The first work to recognize and exploit the value of reinitialization was by Chopp (1993) who used a direct approach.

There are several ways to perform this step. One, of course, is a straightforward approach; simply stand at each computational mesh point and find the signed distance to the front; however, this can be time-consuming. A different technique was introduced by Sussman et al (1994) based on an observation of J.M. Morel. Its virtue is that the level set function is reinitialized without explicitly finding the zero level set; the idea in this approach is to iterate on the equation

$$\phi_t = \text{sign}(\phi)(1 - |\nabla\phi|), \quad (14)$$

until convergence is reached, and the converged result will approximate the signed distance function. It should be noted that when solving Eqn. 14 the reinitialization starts at the interface and moves outwards. Sussman & Fatemi(1999) and Russo & Smereka (2000a) have made improvements in computing solutions to Eqn. 14. Another approach which also does not require explicitly finding the interface comes from running the time-dependent level set method forwards and backwards in time with unit speed, and measuring the crossing times at each grid point, which is then equivalent to finding the signed distance; for details, see (Sethian 1994, Sethian 1996b).

An efficient approach for reinitialization problems is obtained through the use of fast, Dijkstra-like methods to solve the Eikonal equation. Taking an optimal control minimization perspective, Tsitsiklis (1995) decoupled a control theoretic discretization to develop the first such one-pass Dijkstra-like viscosity-satisfying $O(N \log N)$ method for solving the Eikonal equation. By examining the limiting case of Narrow Band Methods (Adalsteinsson & Sethian 1995a) as the bandwidth went to one cell, Sethian developed “Fast Marching Methods” (Sethian 1996a, Kimmel & Sethian 1998, Sethian 1999b), which are Dijkstra-like viscosity-satisfying $O(N \log N)$ finite difference schemes based on upwind hyperbolic operators to approximate the gradient; this approach was used to obtain higher order schemes and schemes on unstructured meshes. It was later seen that a first order version yields the same quadratic update as Tsitsiklis’ optimal control approach. We shall not go into details here and refer the interested reader to the above references; see Helmsen (1996) for a comparison of a similar approach with volume-of-fluid techniques and Sethian & Vladimirsky (2001) for an extension of these Dijkstra-like ideas to anisotropic front propagation and general optimal control.

Armed with these techniques, Adalsteinsson & Sethian (1999) extended the fast methodology to allow the construction of solutions to the extension veloc-

ity equation. The basic idea is to replace the derivatives in Eqn. 12 with upwind operators. In the same manner that Fast Marching Methods systematically construct the signed distance function by marching the solution away from the interface, their approach uses the newly constructed signed distance values to systematically march the extension velocity values themselves away from the values prescribed on the interface.

As an example of a first order technique, assume that $(i + 1, j)$ and $(i, j - 1)$ are the points that are used in updating the distance; if v is the new extension value, it then has to satisfy an upwind version of Eqn. 12, namely

$$\left(\frac{\phi_{i+1,j}^{\text{temp}} - \phi_{i,j}^{\text{temp}}}{h}, \frac{\phi_{i,j}^{\text{temp}} - \phi_{i,j-1}^{\text{temp}}}{h} \right) \cdot \left(\frac{F_{i+1,j} - v}{h}, \frac{v - F_{i,j-1}}{h} \right) = 0.$$

Since $(i + 1, j)$ and $(i, j - 1)$ are known, F is defined at those points, and this equation can be solved with respect to v to produce the extension velocity.

4.4 Additional Numerical Comments and Recent Developments

There are some additional issues involved in the practical implementation of level set methods. To begin, one should try to steer clear of reinitializing too often, since reinitialization tends to generate some error in the position of the front, and these errors can lead to inaccuracy. Second, the use of extension velocities which satisfy the above equation have the considerable virtue that the signed distance function is maintained; this greatly helps avoid unnecessary mass loss during long calculations. Third, poor programming of reinitialization schemes, adaptive strategies and extension schemes can easily render an efficient algorithm inefficient. We refer the interested reader to the above references for details.

We note several recent developments on level set methods. First, in a series of papers, Strain (1999a, 1999b, 1999c) has developed semi-Lagrangian level set methods. Work on triple points and their motion was developed by Bence et al (1994); Smith et al (2001) have made some recent contributions using a projection view to automatically enforce a seamless level set representation with no fix required. A highly accurate way of reinitializing level set functions using bicubic splines was introduced and developed recently by Chopp (2001). Finally we mention that Burchard et al (2001) have developed a level set method for moving curves in 3 dimensions using two level set functions.

4.5 Advantages and Disadvantages of Level Sets

In addition to level set methods, other choices for interface propagation include front tracking (see, for example, Glimm et al 2000 and Tryggvason et al 2001), volume-of-fluid (see, for example, Scardovelli & Zaleski 1999), and phase field methods (see, for example Lowengrub & Truskinovsky 1998)

While phase field methods and level set methods have similarities, there is a non-trivial difference. In level set methods, the choice of level set function is somewhat arbitrary. In phase field methods, the exact profile of the phase

function is important in obtaining the correct interface motion. Advantages of both phase field and level set methods include: (1) they are able to compute geometric quantities easily, (2) many codes can be converted from two to three dimensions quite quickly (this may be more time-consuming for front tracking and volume of fluid methods), and (3) both methods handle topology changes easily. However, we note an important caveat: unresolved flows can exhibit a merger or break up that may not be physical.

In phase field representations, the phase function changes quickly near the interface and hence must be well resolved. As a consequence one needs a large number of grid points near the interface. In some special situations, recent developments in phase field asymptotics have improved this situation (Karma & Rappel 1995). In problems such as the Stefan problem (see, for example, Wheeler et al 1993) and binary alloys (see, for example, Warren & Boettinger 1995) phase field methods have certain aspects which make them preferable to level set methods. A level set approach would require solving the heat equation in complex domain with Dirichlet boundary conditions on the interface, then computing the jump in the normal derivative of the temperature and then extending this to the region around the front. None of this is necessary in a phase field approach, but phase field methods have difficulties of their own. First one must develop a phase field model for a given sharp interface model, then obtain a relationship between the parameters in the phase field model and the sharp interface model. We note that the development of this relation typically involves a nontrivial asymptotic analysis.

One considerable advantage of volume-of-fluid methods in fluid interface simulations is that they conserve mass well. Nonetheless, spurious bubbles and drops may be created (Lafaurie et al 1994), the reconstruction of the interface from the volume fractions are not simple, and computation of geometric quantities such as curvature is not straightforward. Recent work of Bourlioux (1995) and Sussman & Puckett (2000) have combined the best of volume-of-fluid methods and level set methods.

The principle advantage of front tracking algorithms is their inherent accuracy, in part due to the ability to use a large number of grid points on the interface. In addition, topological changes do not occur without explicit action, and hence unphysical numerical reconnection does not occur. For multiphase flow problems, front tracking methods provide accurate and robust solutions. Two major handicaps include the difficulty of including topological change without additional work, and, for geometric problems, issues of numerical instabilities as discussed in Sethian (1985) and Osher & Sethian (1988). In some cases, this instability can be removed by repeatedly re-parameterizing the interface.

We point out that front tracking, volume-of-fluid and level set methods are all sharp interface methods. This indicates that at topology changes the underlying velocity field must lose smoothness and uniqueness of particle trajectories is lost. In level set and volume-of-fluid methods this issue is dealt with by using viscosity solutions. In the case of front tracking this is handled by numerical surgery. This issue is not present with phase field methods since the equation of motion for the phase function is not a hyperbolic equation. It is not clear that any of these

approaches is physically correct at a topological change.

5 TWO-PHASE FLOWS

One very important class of free interface problems occurs with two immiscible and incompressible fluids such as air and water at low Mach numbers. This type of problem has been computed using a number of approaches, including front tracking and volume-of-fluid. In this section we shall describe how to compute the motion of two immiscible fluids that are governed by the incompressible Navier-Stokes equation using level set methods as introduced by Sussman et al (1994). Our starting point will be the equations of motion and the boundary conditions:

$$\begin{aligned} \rho_\ell \frac{D\mathbf{u}_\ell}{Dt} &= -\nabla p_\ell + 2\mu_\ell \nabla \cdot \mathcal{D}_\ell + \rho_\ell \mathbf{g}, & \nabla \cdot \mathbf{u}_\ell &= 0, & \mathbf{x} \in \text{the liquid}, \\ \rho_g \frac{D\mathbf{u}_g}{Dt} &= -\nabla p_g + 2\mu_g \nabla \cdot \mathcal{D}_g + \rho_g \mathbf{g}, & \nabla \cdot \mathbf{u}_g &= 0, & \mathbf{x} \in \text{the gas}, \end{aligned} \quad (15)$$

where \mathbf{u} is the velocity, p is the pressure, ρ is the density, and μ is the viscosity of the fluid. The subscripts ℓ and g denote the liquid and the gas phase, respectively. D/Dt is the material derivative, \mathcal{D} is the rate of deformation tensor, and \mathbf{g} is the acceleration due to gravity. The boundary conditions at the interface, Γ , between the phases are:

$$(2\mu_\ell \mathcal{D} - 2\mu_g \mathcal{D}) \cdot \mathbf{n} = (p_\ell - p_g + \sigma \kappa) \mathbf{n} \quad \text{and} \quad \mathbf{u}_\ell = \mathbf{u}_g, \quad \mathbf{x} \in \Gamma, \quad (16)$$

where \mathbf{n} is the unit normal of the interface drawn outwards from the gas to the liquid, $\kappa = \nabla \cdot \mathbf{n}$ is the curvature of the interface, and σ is the coefficient of surface tension. For more details see, for example, Batchelor (1967).

Now we make two definitions, namely

$$\mathbf{u} = \begin{cases} \mathbf{u}_\ell & \mathbf{x} \in \text{the liquid} \\ \mathbf{u}_g & \mathbf{x} \in \text{the gas}, \end{cases} \quad \text{and} \quad \rho = \begin{cases} \rho_\ell & \mathbf{x} \in \text{the liquid} \\ \rho_g & \mathbf{x} \in \text{the gas}. \end{cases}$$

μ is defined in analogous fashion. The system of equations given by Eqn. 15 and the boundary condition Eqn. (16) can be combined into following:

$$\rho \frac{D\mathbf{u}}{Dt} = -\nabla p + \nabla \cdot (2\mu \mathcal{D}) - \sigma \kappa \delta(d) \mathbf{n} + \rho \mathbf{g}, \quad \nabla \cdot \mathbf{u} = 0, \quad \mathbf{x} \in \Omega \quad (17)$$

where Ω is the domain containing both fluids and δ is the Dirac delta function. d is the signed distance function from the interface; which is defined as follows: at a point \mathbf{x} in liquid d is the distance to closest point on the interface. In the gas d is the negative of this quantity. The idea of incorporating surface tension as a force concentrated on the interface appears to be due to Peskin (1977). The form above, however, comes from Unverdi & Tryggvason (1992). A derivation of Eqn. 17 can be found in Chang et al (1996) and Smereka (1996).

5.1 Density Weighted Divergence-Free Projection

In order to enforce the incompressibility condition, we must introduce the density weighted divergence-free projection operator. To begin we let $\rho(\mathbf{x})$ be a density function and $\mathbf{f}(\mathbf{x})$ be an arbitrary vector field defined on Ω . Then the weighted divergence-free projection of \mathbf{f} , denoted \mathbf{u} , is defined as

$$\mathbf{u} = \frac{1}{\rho} \nabla p - \mathbf{f}, \quad (18)$$

with $\mathbf{u} \cdot \mathbf{n} = 0$ on $\partial\Omega$. Since $\nabla \cdot \mathbf{u} = 0$, then p must satisfy the following elliptic equation:

$$\nabla \cdot \left(\frac{1}{\rho} \nabla p \right) = \nabla \cdot \mathbf{f}, \quad \text{with} \quad \frac{\partial p}{\partial n} = \mathbf{f} \cdot \mathbf{n} \quad \text{on} \quad \partial\Omega. \quad (19)$$

We shall denote the weighted projection by P_ρ ; therefore $\mathbf{u} = P_\rho(\mathbf{f})$. We observe that $P_\rho\left(\frac{1}{\rho} \nabla q\right) = 0$ where q is any scalar field. It is then clear that we can eliminate the pressure from Eqn. 17 by applying the weighted divergence-free projection operator.

5.2 Level Set Formulation

We introduce the level set function ϕ , the zero level set of which is the gas-liquid interface:

$$\Gamma = \{\mathbf{x} | \phi(\mathbf{x}, t) = 0\}.$$

We also take $\phi < 0$ in the gas region and $\phi > 0$ in the liquid region. As discussed earlier, the unit normal and curvature on the interface liquid and can be easily expressed in terms of $\phi(\mathbf{x}, t)$. The density and viscosity are constant in each fluid and take on two different values depending on the sign of ϕ , and hence we may write

$$\rho(\phi) = \rho_g + (\rho_\ell - \rho_g)H(\phi) \quad \text{and} \quad \mu(\phi) = \mu_g + (\mu_\ell - \mu_g)H(\phi) \quad (20)$$

where $H(\phi)$ is the Heaviside function given by

$$H(\phi) = \begin{cases} 0 & \text{if } \phi < 0 \\ \frac{1}{2} & \text{if } \phi = 0 \\ 1 & \text{if } \phi > 0. \end{cases}$$

Since the interface moves with the fluid particles, the evolution of ϕ is then given by

$$\frac{\partial \phi}{\partial t} + \mathbf{u} \cdot \nabla \phi = 0. \quad (21)$$

5.3 Thick Interfaces

The sharp changes in ρ across the front can present numerical difficulties. To alleviate these problems we shall give the interface a fixed thickness proportional

to the spatial mesh size. This allows us to replace $\rho(\phi)$ by a smoothed density, $\rho_\varepsilon(\phi)$, which is given by Eq. 20 with H replaced by

$$H_\varepsilon(\phi) = \begin{cases} 0 & \text{if } \phi < -\varepsilon \\ \frac{1}{2}[1 + \frac{\phi}{\varepsilon} + \frac{1}{\pi} \sin(\pi\phi/\varepsilon)] & \text{if } |\phi| \leq \varepsilon \\ 1 & \text{if } \phi > \varepsilon. \end{cases} \quad (22)$$

In this way the interface now has a thickness of approximately $\frac{2\varepsilon}{|\nabla\phi|}$. The smoothed or mollified delta function is

$$\delta_\varepsilon(\phi) = \frac{dH_\varepsilon}{d\phi}. \quad (23)$$

If we replace ρ , μ and δ by their smoothed counterparts then Eqn. 17 becomes:

$$\frac{D\mathbf{u}}{Dt} = \frac{1}{\rho_\varepsilon(\phi)} (-\nabla p + \nabla \cdot (2\mu_\varepsilon(\phi)\mathcal{D}) - \sigma\kappa\delta_\varepsilon(\phi)\nabla\phi) + \mathbf{g} \quad (24)$$

The Navier-Stokes equations for two-fluid flows was written in similar form by Unverdi & Tryggvason (1992). The form of the surface tension we use here is due to Brackbill et al (1992) and Chang et al (1996).

In our algorithm the front must have a uniform thickness, consequently we must have $|\nabla\phi| = 1$ when $|\phi| \leq \varepsilon$. A function that has this property is a signed distance function near the front. It is clear that we can initialize ϕ in this way but under the evolution of Eqn. 21 it will not remain so. Therefore, one must reinitialize ϕ so that it remains a distance function near the front as the computation proceeds. For more details the reader is referred to Sussman et al (1994, 1997, 1998, 1999) and Sethian & Yu (2002).

5.4 Numerical Issues

There are three main numerical issues when computing these equations. They are the projection step, spatial discretization, and time discretization.

5.4.1 The Projection Operator

One crucial step in the numerical simulation of incompressible flows is the computation of the projection step. This entails enforcing the incompressibility condition ($\nabla \cdot \mathbf{u} = 0$). Projection methods for variable density flows are well-studied techniques. Computing the projection step entails first solving an elliptic equation with Neumann boundary conditions Eqn. 19 and then computing a gradient Eqn. 18. In Chorin's formulation (Chorin, 1968) pressure and velocity are defined at nodes and central differences are used. Chorin then chooses the stencil for Eqn. 18 and Eqn. 19 so that the velocity field is exactly discretely divergence free; hence this is called an exact projection. The stencil for this exact projection is an expanded five point stencil. This can give rise to numerical difficulties. One way to remove some of these difficulties is to replace the expanded 5 point stencil

by the regular 5 point stencil (Lai 1993). The resulting velocity field is only approximately discretely divergence free. This method is found to work well except when there are very large differences in density between the two phases as in air and water (Sussman 2002a).

Another approach is to use the marker and cell (MAC) projection (Harlow & Welch 1965). In this formulation the pressure is defined at cell centers and velocities are defined at cell edges. Therefore the different velocity components are defined on different grids. In this approach the velocity field can be made discretely divergence free. However, as pointed out by Almgren et al (1996), since the velocity components live on different grids the implementation of high order upwind methods for the convection terms is difficult.

Bell et al (1989) introduce a projection method that is an exact projection, has compact stencil and velocity variables live on the same grid. This projection method was extended to variable density flows by Bell & Marcus (1992). In the context of level set computations, Sussman et al (1994,1997,1998) used this formulation for two-dimensional and three-dimensional axisymmetric flows. This projection method was found to behave extremely well. Its disadvantage is that it is based on a stream function formulation and consequently becomes more expensive in three dimensions. This is because one needs to use a vector potential and solve three elliptic equations. Nevertheless, given the advantages that this approach offers, it might be worth exploring this method for three-dimensional two-phase flow problems.

Almgren et al (1996) and Puckett et al (1997) introduce a new approach for computing the projection operator. In this approach, the pressure is defined at the cell corners and the velocities are defined at the cell centers. The authors use an approximate projection method resulting in a compact 9-point stencil for the Laplacian. Since the velocities are defined on the same grid, with relative ease one can develop high order upwind methods for the convection terms. This approach also has advantages when using adaptive mesh refinement (Almgren et al 1998). Sussman et al (1999) and Sussman & Puckett (2000) have adopted this method for their computations.

5.4.2 Spatial Discretization

There are several different types of terms that need to be discretized. First, we consider the convective terms given by $\mathbf{u} \cdot \nabla \mathbf{u}$ and $\mathbf{u} \cdot \nabla \phi$. The basic strategy is upwinding; one simple upwind approach is given by

$$c \frac{\partial u}{\partial x} = \begin{cases} c \frac{u_{i-1} - u_i}{h} & \text{if } c > 0 \\ c \frac{u_{i+1} - u_i}{h} & \text{if } c < 0. \end{cases} \quad (25)$$

The above algorithm is stable; unfortunately it is only first order accurate. One successful approach to providing high order accurate approximations for these convective terms is to use techniques from numerical algorithms for conservation

laws. The essential idea is to use a larger stencil to gain accuracy while ensuring that the conservation property and upwinding are maintained. In addition these schemes are designed to minimize unphysical oscillations. See, for example, Colella (1985,1990), Osher & Sethian (1988), Osher & Shu (1991), Shu & Osher (1987,1988), and Harten et al (1987a,1987b). Even though there is no shock formation in incompressible fluids, these schemes have been found to quite useful in level set computations. In particular they suppress unphysical oscillations that can occur near the interface.

Both the viscosity and surface tension terms are approximated using central difference approximations. Additionally, we note that the projection of a delta function is required in the evaluation of the surface tension term. The most singular part of this term is a gradient term which indicates that it should be naturally eliminated by the projection operator. There are two ways to make sure this happens correctly. The first approach is to rewrite the surface tension term and explicitly remove the gradient term (Sussman et al 1994, 1998). The second approach is to make sure that the discrete form of the projection operator eliminates discrete gradient terms.

5.4.3 Temporal Discretization

There are two basic methods to advance in time. The first is to apply the projection operator to Eqn. 24, thereby eliminating the pressure term, view it as large system of ordinary differential equations (ode) and use standard ode solvers. This was the approach taken by Sussman et al (1994,1997,1998). Its advantage is that one can obtain high order methods (in time) easily. The disadvantage is that, if the viscosity is large enough, the method can become stiff and one must use small time steps to maintain stability. Another approach is to use a fractional step method (Chorin 1969, Kim & Moin 1985) and solve the viscous term implicitly. This approach can lead to second order accurate schemes but it seems difficult to extend them to higher order. A new fractional step was developed by Bell et al (1989) to allow the incorporation of second order Godunov methods. Their approach was adopted by Puckett et al (1997), Sussman et al (1999) and Sussman & Puckett (2000).

5.5 Recent Developments

Zhao et al (1996) developed level set technique for multiphase flows where the equations of motion can be deduced from a variational formulation. The fact the two phases cannot occupy the same physical location was incorporated as a constraint. This idea was used to study the behavior of bubbles and drops by Zhao et al (1998). The authors considered only surface tension effects, and the time evolution of the bubbles and drops are only valid if the surface tension effects dominate all other physical effects such as fluid inertia, viscosity, and internal circulation; nonetheless, the obtained equilibrium shapes are physically accurate.

In the area of incompressible two phase flows there have been some interesting recent developments. One of these concerns mass loss. One of the problems faced with level set methods for incompressible two phase flows is that they tend to lose mass, despite serious efforts (Sussman et al 1998,1999). One recent improvement in this direction is the development of a coupled level-set/volume-of-fluid method by Bourlioux (1995) and Sussman & Puckett (2000). An example of two rising bubbles from Sussman & Puckett (2000) is shown in Figure 2. This method seems to conserve mass almost as well as volume-of-fluid methods without the creation of artificial drops and bubbles (called flotsam by the volume of fluid practitioners, see, for example, the review article by Scardovelli & Zaleski 1999). In addition, due to the level set representation of the interface, surface tension effects are much easier to incorporate. Overall this seems like an extremely promising method. This method has been used to simulate droplet formation in inkjet printers by Aleinov et al (1999) and compute the wake of a ship by Sussman & Dommermuth (2000). Examples of this work are shown in Figures 3 and 4.

Another development is due to Kang et al (2000). In their formulation they do not smooth the density or viscosity. Instead they keep the interface sharp, and are thus faced with a more difficult elliptic problem; this is then solved with a boundary condition capturing method developed by Liu et al (2000). The work of Liu et al (2000) is closely related to work by Mayo (1992) and Hou et al (1997). Level set methods have been developed for two fluid flows where one of the fluids is compressible and the other is incompressible by Caiden et al (2001) and Sussman (2002b). In addition, Son & Dhir (1998) have developed a level set method for boiling liquids.

Enright et al (2001) have introduced the particle level set method where in addition to the level set function the authors also solve for the motion of a large number of particles that have been “released” near the interface. Since these particles move with the same velocity as the the level set function, they should not cross the zero level set. By checking for particles that cross, due to numerical inaccuracies, authors reconstruct the level set function. Considerable improvement in mass conservation is obtained.

5.6 Compressible Two-Phase Flows

In many applications, two different compressible fluids are separated by a sharp interface; in most cases, the two fluids will have different equations of state. There has been considerable work in this direction using front tracking, see for example, Chern & Colella (1985), Glimm et al (1981,1998,2000) and LeVeque & Shyue (1996). As examples, Glimm et al (1998,2000) have presented some very impressive three-dimensional calculations of the compressible Rayleigh-Taylor instability. Near the interface, Glimm and co-workers introduce ghost cells and solve a Riemann problem at the interface which is then used to fill the ghost cells on either side of the interface. We refer the reader to the references for a series of calculations using these techniques.

Level set methods for compressible flow include the early work by Mulder et al (1992); the authors used the compressible Euler equations with the equation

of state for an ideal gas. A sharp interface was assumed, which separated gases with two different adiabatic exponents, and the Euler equations were amended to include a level set equation written in conservation form. Karni(1994,1996) showed that this algorithm produces unphysical oscillations. She showed that these oscillations arise because discretizations in conservation form fail to give the correct jump conditions at the interface between the two gases. In the case of the compressible Euler equation the pressure should be continuous at the interface, however any discrete conservative formulation will disrupt this jump condition and cause oscillations (see also Abgrall & Karni (2001a).)

To eliminate these oscillations, Karni(1994,1996), made the bold move of giving up the conservative form of the finite difference scheme at the interface between the two gases. The conservation form was maintained elsewhere thus ensuring that shock waves will be computed correctly. Quirk & Karni (1996) used this method to compute the interaction of a shock wave in air with a helium bubble.

An important development that also circumvented these problems is called the ghost fluid method (Fedkiw 1999, Fedkiw et al 1999a). The basic idea of this method is based on the observation, (for the compressible Euler equations) that at interface between the two gases, the normal velocity and pressure are continuous whereas the entropy can be discontinuous. In the ghost fluid method one introduces ghost fluids on either side of the interface. Since pressure and normal velocity are continuous across the interface the ghost fluids have the same pressure and normal velocity of the actual fluid. The entropy of the ghost fluid is determined by extrapolating the entropy across the interface. One then solves the equations of motion using any standard method for conservation laws for both the actual fluid and the ghost fluid. Since the interface is tracked using a level set function, one can use it to determine which fluid is real and which is ghost. In this approach, the entropy is not smeared across the interface and hence pressure oscillations are prevented. We note that this method also does not satisfy conservation near the interface.

Advantages of the ghost fluid method include that it is easy to implement, appears to be robust, and can handle fluid mixtures with extremely different equations of state. The method extends easily to higher space dimensions since one can use velocity extension methods to “fill the ghost cells with the ghost fluid”. We note that rather than solve a Riemann problem at the interface which is then used to fill ghost cells, as was done by Glimm et al (1981, 2001) and discussed above, the ghost fluid method uses extrapolation based on the jump condition at the interface. This extrapolation procedure is easy since the interface has a level set representation, however, the solution of the Riemann problem is not as simple. It should be noted that the application of the ghost fluid method in Fedkiw et al (1999b) requires the solution of a Riemann problem, not to fill ghost cells, but instead to compute shock speeds.

The ghost fluid method has been extended to problems relating to deflagration and combustion by Fedkiw et al (1999b), and more recently Abgrall & Karni (2001b) developed a different approach which has some similarities to the ghost fluid method and has also has been incorporated in a level set framework. Additionally, we note that in its simplest implementation, one must have two copies

of the solution everywhere. However all that is really needed is a ghost fluid in a few cells on either side of the interface. This can be accomplished by using narrow band methods (see Adalsteinsson & Sethian 1995a and Peng et al 1999a).

Finally, we note that there have been a series of combustion calculations using level set methods. In fact, the first coupling of level set methods to projection methods was the cold flame calculations of Zhu & Sethian (1992); here, a single step premixed flame model was assumed in which flame propagation affected the underlying hydrodynamics through expansion, but fluid mechanical effects were not allowed to alter the flame speed. These were followed by the flame holder calculations of Rhee et al (1995), in which the volume expansion along the burning flame front affected the fluid velocity in a chamber through an elliptic source term, which in turn created a pressure field and hydrodynamic field which affected the combustion dynamics. Other level set combustion calculations include the work of Zhu & Ronney (1995).

5.7 Example Application: The Design of Inkjet Printheads

As an example of the applicability of these techniques, we discuss in some detail recent work on using two-phase level set calculations to simulate the fluid dynamics of inkjet printheads. The first such calculation using a combination of level set methods and projection methods in droplet formation in inkjet printers is due to Aleinov et al (1999); there, axi-symmetric three dimensional simulations were performed of the jetting process and we refer the reader to that work.

Here, we discuss in some detail the work of Sethian & Yu (2002) on this problem. As motivation, in Figure 5 we show a schematic design of the nozzle associated with an inkjet printhead; both the geometry and the actual calculation are in fact axisymmetric and the figure is not drawn to scale. Ink is stored in a bath reservoir, and driven through the nozzle in response to a pressure jump at the lower boundary. The dynamics of incompressible flow through the nozzle, coupled to surface tension effects along the air-fluid interface and boundary conditions along the wall act to determine the shape of the interface as it moves. A negative pressure at the lower boundary induces a backflow which causes the bubble to break off, separating and moving through the domain.

The goal is to model this process, capturing the dynamics of the interface motion, the bubble breakage, ejection, downstream motion and formation of satellites. The underlying algorithms should be able to accurately capture two phase flow through an axisymmetric nozzle, handle the complicated topology change of ink droplets, reasonably conserve mass, and work with external models which simulate the ink cartridge, supply channel, and actuator.

The model is based on the Navier-Stokes equations for two-phase incompressible flow in the presence of surface tension and density jumps across the interface separating ink and air, coupled to an electric circuit model which describes the driving mechanism behind the process, and a macroscale contact model which describes the air-ink-wall dynamics. It is important in this simulation that the effects of corners in the body geometry be handled correctly. Consequently, Sethian & Yu (2002) develop an axisymmetric quadrilateral mesh implementation of the

second order projection method, following the implementation formulation given by Bell & Colella (1994), and Trebotich & Colella (2001), with some care taken for the viscosity term; for details, see Sethian & Yu (2002).

5.7.1 Boundary Conditions and Models

On solid walls, we assume that both the normal and tangential components of the velocity vanish (this must be amended at the triple point, which we discuss below). At both inflow and outflow, the formulation allows us to provide either velocity or pressure boundary conditions. Time-dependent inflow conditions are provided by an equivalent circuit model which mimics the charge-driven mechanism which forces ink from the bath into the nozzle.

At the triple point where air and ink meet at the solid wall, several choices are available for the boundary conditions. First, one can choose to enforce the no-slip condition, in which case the triple point will remain fixed. Alternatively, one can choose to enforce some sort of condition which restricts the allowable critical angle; this will cause the triple point to move. A third option is to relax the no-slip condition in the neighborhood of the triple point once the critical angle is exceeded; the idea here is to allow the local flow at the triple point to quickly accelerate whenever the critical angle is exceeded (see, for example Bertozzi 1998).

This leads to a macroscopic contact model based on the level set concept, namely

$$\mathbf{u} \cdot \mathbf{t} = W(\phi)G(\theta, \theta_a, \theta_r, \mathbf{u}_\Delta \cdot \mathbf{t}) . \quad (26)$$

In the above, \mathbf{t} is the unit tangent vector, θ is the contact angle made by the liquid-air interface and the liquid-solid boundary, and θ_a, θ_r are the advancing and receding critical contact angles. The contact angle θ is measured at a distance δl from the contact point. The advancing critical contact angle is the maximum angle for the contact point to stay fixed. If $\theta \geq \theta_a$, the contact point is allowed to slide toward the air side; the opposite is applied to the receding critical contact angle θ_r (usually $\theta_a > \theta_r$.) Finally, W is a weighting function which sets the the slipping velocity equal to zero outside a range of ϵ_{cnt} from the contact point and to make the transition from no-slip to slipping condition smoothly, while the function G sets the slipping velocity to be bigger than the tangential velocity at a distance from the contact point whenever the critical angles are exceeded. This will provide a restoring force to accelerate the contact point so that the contact angle will return sooner to the critical angle.

To drive the fluid dynamics, the formation of an ink droplet in a piezo inkjet print head is controlled by a piece of piezoelectric PZT actuator which pushes and then pulls the ink. Since only the input voltage is known, suitable boundary conditions are provided by an electric circuit model whose input is the driving voltage and output is the inflow velocity or pressure to the nozzle. A typical driving voltage pattern and a typical inflow pressure are as shown in Figures 6a and 6b.

5.7.2 Results of Numerical Simulation

For the inkjet simulation, consider a typical nozzle as in Figure 5. The diameter is 26 microns at the opening and 65 microns at the bottom. The length of the nozzle opening part, where the diameter is 26 microns, is 20.8 microns. The slant part is 59.8 microns and the bottom part is 7.8 microns.

The inflow pressure is given by an equivalent circuit which simulates the effect of the ink cartridge, supply channel, vibration plate, PZT actuator, applied voltage, and the ink inside the channel and cartridge. The input voltage is given by Figure 6a. The corresponding inflow pressure is as shown in Figure 6b. The outflow pressure at the top of the solution domain is set to zero.

The solution domain was chosen to be $\{(r, z) | 0 \leq r \leq 39\mu m, 0 \leq z \leq 312\mu m\}$. The contact angle was assumed to be 90° all the time and the initial meniscus is assumed to be flat and 2.6 microns under the nozzle opening. For the purpose of normalization, the nozzle opening diameter (26 microns) is chosen to be the length scale and $6 m/sec$ to be the velocity scale. The normalized solution domain is hence $\{(r, z) | 0 \leq r \leq 1.5, 0 \leq z \leq 8\}$. Since the density, viscosity, and surface tension of ink are approximately $\rho_1 = 1070 Kg/m^3$, $\mu_1 = 3.34 \times 10^{-3} Kg/m \cdot sec$, and $\sigma = 0.032 Kg/sec^2$, this yields the non-dimensional parameters $Re = 50$ and $We = 31.3$. Simulation results are shown in Fig. 7; see Sethian and Yu (2002) for details and additional calculations.

6 PROBLEMS IN MATERIAL SCIENCE

In addition to fluid mechanics calculations, level set methods have been applied to many problems in material science. As examples, solidification problems modeled by the Stefan problem have been computed using level set methods by Sethian & Strain (1992), Chen et al (1997), Kim et al (2000), Gibou et al (2002), and Chopp & Dolbow (2001). In addition the spiral mode of crystal growth has been studied by Smereka (2000). Chopp & Sethian (1999) and Smereka (2003) have developed level set methods for motion by surface diffusion. In addition problems relating to etching, deposition and lithography have been put into a level set frame work by Adalsteinsson & Sethian (1995a, 1995b, 1997) and Baumann et al (2001). Continuum models for island dynamics in epitaxial growth have been implemented using level set methods by Caffisch et al (1999), Chen et al (2000) and Chopp (2000). Sukumar et al (2001) have combined finite element methods with level set ideas to develop computational tools to study defects in materials. Below, we examine a problem concerning growth of faceted polycrystalline thin films where level set methods have also been quite useful.

6.1 Example Application: Faceted Polycrystalline Thin Films

In many situations thin films are neither single crystals nor amorphous, instead, they are composed of a mixture of tiny perfect crystals. Each crystal is different from the others in the film only by its orientation. These thin films are called

polycrystalline and are used in a large number of applications. Typically the orientations have two out-of-plane angles and an in-plane angle. The out-of-plane angles measure how much the crystal normal tilts from the substrate normal and the in-plane angle records the amount of in-plane rotation.

A polycrystalline film with a narrow distribution of out-of-plane angles and a very broad distribution of in-plane angles is said to have a good or strong fiber texture. Biaxial texture refers to both the in-plane and out-of-plane grain orientation distributions. A polycrystalline film with good biaxial texture will have narrow distribution functions for both in-plane and out-of plane orientations. A polycrystalline film with good biaxial texture could be thought of as almost a single crystal film.

One of the simplest models used to understand texture evolution was developed by van der Drift (1967). In this model the polycrystalline thin film is composed of completely faceted crystals. Each crystal has a prescribed set of normals and normal speeds. When two crystals grow into each other, their common interface stops growing. The texture evolution is determined by the complex interaction between the crystals. This model has been implemented in two space dimensions (see, for example, Paritosh et al 1999) using front tracking ideas but its extension to three space dimensions seems completely intractable. Using level set methods, Russo & Smereka (2000b) have been able to provide a numerical algorithm to solve the van der Drift model in three dimensions. In this problem the main advantage of level sets is not that they handle topological changes but instead that they are particularly adept at computing geometric quantities.

Let us now outline the derivation of this model. We assume the speed of the interface is a known function of the normal direction; the location of the interface can then be determined from

$$\dot{\mathbf{x}} = \gamma(\mathbf{n})\mathbf{n}. \quad (27)$$

This equation has a long history and the reader is referred to the articles by Taylor et al (1992) and Peng et al (1999b) and the references therein. The important discovery made by Wulff (1901) and Frank (1958) is that if $\gamma(\mathbf{n})$ is smooth and convex then an initial smooth curve will remain smooth. On the other hand, if is not convex then corners and facets develop. In both cases the asymptotic shape is given by the Wulff shape which is the Legendre transform of γ or equivalently the inner convex hull of γ . This was proved by Soravia (1994) and Osher & Merriman (1997). As pointed out by Peng et al (1999b) the development of a facet is analogous to the formation of a shock. The level set version of Eqn. 27 is

$$\frac{\partial \phi}{\partial t} + \gamma \left(\frac{\nabla \phi}{|\nabla \phi|} \right) |\nabla \phi| = 0 \quad (28)$$

Osher & Merriman (1997) prove that as $t \rightarrow \infty$ the zero level set of ϕ will tend to the Wulff shape of γ . Peng et al (1999b) compute numerical solutions to Eqn. 28.

In order to use Eqn. 28 for the van der Drift model, two hurdles need to be overcome. First, for a given set of normals and normal velocities we must find γ . This is a type of inverse Legendre transform problem. Second, we need to develop a method to enforce the constraint which requires that where two crystals have

grown into each other (a grain boundary) the interface does not move. This was accomplished by Russo & Smereka (2000b). In this approach, each crystal needs to have its own level set function. For problems with a large number of seeds this becomes very expensive both in terms of computer time and memory, to this end Russo & Smereka (2002) developed a narrow band method with dynamic memory allocation for multiple level set functions. In addition, the narrow band has an active part and an inactive part. The active part is where the crystals are growing and the inactive part is where the crystals have grown into each other and no further growth occurs. The inactive parts are removed from memory on stored on the hard drive. In this way, one can compute problems with over 200 level set functions on grids as big as $350 \times 350 \times 1200$.

Li et al (2002) have used this method to study diamond films. Depending on growth conditions, diamond can grow as a cube, or an octahedron or a 14-sided polyhedron (a cube with the corners replace by facets) In Figure 8, results are shown for the growth of diamond film when the diamond crystals are growing in the cubic mode. As the film grows, the corners dominate. Figure 9 presents results in the case when the diamond crystals are 14-sided. In this case the (001) facets of diamond begin to dominate. In both cases the film develops a strong fiber texture.

7 CONCLUSIONS

We note the obvious: no review can be complete, and much valuable work has been reluctantly omitted. We refer the reader to the reviews listed earlier for a more complete view of this evolving field.

ACKNOWLEDGMENTS

JS thanks D. Adalsteinsson, D. Chopp, R. Fedkiw, R. Malladi, M. Minion, G. Tryggvason, and A. Vladimirovsky for helpful discussions, and acknowledges support from the Applied Mathematical Science subprogram of the Office of Energy Research, U.S. Department of Energy, under Contract Number DE-AC03-76SF00098, and the Division of Mathematical Sciences, National Science Foundation. PS thanks R. Fedkiw, S. Karni, and M. Sussman for helpful discussions and acknowledges support from NSF through a Career award and NSF and DARPA through the VIP initiative.

Literature Cited

1. Abgrall R, Karni, S. 2001a. Computation of compressible multifluids. *J. Comput. Phys.* 169 594-623
2. Abgrall R, Karni S. 2001b. Ghost Fluids for the Poor: A single fluid algorithm for multi-

- fluids. in *Hyperbolic problems: theory, numerics, applications: eighth international conference, Magdeburg, Feb-Mar. 2000.* (ed. H. Freistühler and G. Warnecke) Birkhäuser, Berlin.
3. Adalsteinsson D, Sethian JA, 1995. A Fast Level Set Method for Propagating Interfaces, *J. Comp. Phys.* 118 2 269–277
 4. Adalsteinsson D, Sethian JA, 1995. A Unified Level Set Approach to Etching, Deposition and Lithography I: Algorithms and Two-dimensional Simulation *J. Comput. Phys.* 120 1 128–144
 5. Adalsteinsson D, Sethian JA. 1995. A Unified Level Set Approach to Etching, Deposition and Lithography II: Three-dimensional Simulations *J. Comput. Phys.* 122 2 348–366
 6. Adalsteinsson D, Sethian JA, 1997. A Unified Level Set Approach to Etching, Deposition and Lithography III: Complex Simulations and Multiple Effects *J. Comput. Phys.* 138 1 193–223
 7. Adalsteinsson D, Sethian, JA. 1999. The Fast Construction of Extension Velocities in Level Set Methods, *Journal Computational Physics* 148 2-22
 8. Aleinov I, Puckett EG, Sussman M. 1999. Formation of Droplets in Micro-scale Jetting Devices. in Proceedings of the 3rd ASME/JSME joint fluids engineering conference, July (1999)
 9. Almgren AS, Bell JB, Colella P, Howell L, Welcome M. 1998. A conservative adaptive projection method for the variable density incompressible Navier-Stokes equations. *J. Comput. Phys.* 142 1-46
 10. Almgren AS, Bell JB, Szymczak WB. 1996. A numerical method for the incompressible Navier-Stokes equations based on an approximate projection. *SIAM J. Sci. Comput.* 17 358–69
 11. Batchelor GK. 1967 *An introduction to fluid dynamics*. Cambridge: Cambridge Univ. Press.
 12. Baumann FH, Chopp DL, de la Rubia TD, Gilmer GH, Greene JE, Huang H, Kodambaka S, O’Sullivan P, Petrov I. 2001. Multiscale modeling of thin-film deposition: Applications to Si device processing *MRS Bulletin* 26 182–9
 13. Bell JB, Colella PC. 1994. A Projection Method for Viscous Incompressible Flow on Quadrilateral Grids. *AIAA Journal*, 32,(10).
 14. Bell JB, Colella P, Glaz HM. 1989. A second order projection method for incompressible

- Navier-Stokes equations. *J. Comput. Phys.* 85 257–83
15. Bell JB, Marcus DL. 1992. A second order projection method for variable density flows. *J. Comput. Phys.* 101 334–48
 16. Bertozzi, A. 1998. The Mathematics of Moving Contact Lines in Thin Liquid Films, *Notices of the American Mathematical Society*. p. 689, June-July.
 17. Bourlioux A, 1995. A coupled level-set volume-of-fluid for tracking material interfaces. In *Proceedings of the 6th International Symposium on Computational Fluid Dynamics*, Lake Tahoe CA.
 18. Brackbill JU, Kothe DB, Zemach C. 1992. A continuum method for modeling surface tension. *J. Comput. Phys.* 100 335–54
 19. Burchard P, Cheng LT, Merriman B, Osher S. 2001. Motion of curves in three spatial dimensions using a level set approach. *J. Comput. Phys.* 170 720–41
 20. Caffisch RE, Gyure MF, Merriman B, Osher SJ, Ratsch C, Vvedensky DD, Zinck JJ. 1999. Island dynamics and the level set method for epitaxial growth, *App. Math. Lett.* 12 13–22
 21. Caiden R, Fedkiw R, Anderson C. 2001. A numerical method for two phase flow consisting of separate compressible and incompressible regions. *J. Comput. Phys.* 166 1-27
 22. Chang YC, Hou TY, Merriman B, Osher SJ. 1996. A level set formulation of Eulerian interface capturing methods for incompressible fluid flows. *J. Comput. Phys.* 124 449–64
 23. Chen S, Merriman B, Kang M, Caffisch RE, Ratsch C, Cheng L, Gyure M, Fedkiw RP, Anderson CR, Osher SJ. 2000. Level set method for thin film epitaxial growth. *J. of Comp. Phys.* 167 475–500
 24. Chen S, Merriman B, Osher S, Smereka P. 1997, A simple level set method for solving Stefan problems. *J. Comput. Phys.* 135 8–29
 25. Chern IL, Colella P. 1987. A conservative front tracking method for hyperbolic conservation laws. LLNL Rep. No. UCRL-97200, Lawrence Livermore National Laboratory, Livermore CA.
 26. Chopp DL. 1993. Computing minimal surfaces via level set curvature flow. *J. Comput. Phys.* 106 77-91
 27. Chopp DL. 2000. A level-set method for simulating island coarsening. *J. Comput. Phys.* 162 104–122.

28. Chopp DL. 2001. Some improvements of the fast marching method. *SIAM J. Sci. Comp.* 23 1 230–244.
29. Chopp DL, Dolbow JE, 2001. A hybrid extended finite element/level set method for modeling phase transitions. *International Journal of Numerical Methods for Engineering*, to appear.
30. Chopp DL, Sethian JA. 1999 Motion by intrinsic Laplacian of curvature *Interfaces and Free Boundaries* 1 107–23
31. Chorin AJ. 1968. Numerical solution of the Navier-Stokes equations. *Math. Comput.* 22 745–62
32. Chorin AJ. 1969. On convergence of discrete approximations to Navier-Stokes equations *Math. Comput.* 23 341–53
33. Colella P. 1985. A direct Eulerian MUSCL scheme for gas dynamics. *SIAM J. Sci. Stat. Comput.* 6 104–117
34. Colella P. 1990. A multidimensional second order Godunov scheme for conservation laws. *J. Comput. Phys.* 87 171–200
35. Crandall MG, Lions PL. 1983. Viscosity Solutions of Hamilton–Jacobi Equations. *Tran. AMS*, 277, pp. 1–43.
36. Crandall MG, Lions PL. 1984. Two Approximations of Solutions of Hamilton-Jacobi Equations, *Math. Comp.*, 167, 43, pp. 1–19.
37. Enright D, Fedkiw RP, Ferziger J, Mitchell I. 2001. A hybrid particle level set method for improved interface capturing. preprint.
38. Fedkiw, R. 1999. The ghost fluid method for discontinuities and interfaces, In: Godunov Methods: Theory and Applications, Oxford, UK
39. Fedkiw RP, Aslam T, Merriman B, Osher SJ. 1999a. A non-oscillatory Eulerian approach to interfaces in multimaterial flows (the ghost fluid method). *J. Comput. Phys.* 152 457-492
40. Fedkiw RP, Aslam T, Xu SJ. 1999b. The ghost fluid method for deflagration and detonation discontinuities *J. Comput. Phys.* 154 393-427
41. Frank FC 1958 On the kinematic theory of crystal growth and dissolution processes. in *Growth and Perfection of Crystals* ed. RH Doremus, BW Roberts, D Turnbull, John Wiley, New York.

42. Gibou F, Fedkiw R, Cheng LT, Kang M. 2002. A second order accurate symmetric discretization of the Poisson equation on irregular domains”, *J. Comput. Phys.* (in press)
43. Glimm J, Xiao LL, Liu Y, Zhao N. 2001. Conservative front tracking and level set algorithms. *Proc. Nat. Acad. Sci.* 98 14198–201
44. Glimm J, Grove JW, XL Li, Shyue KM, Zeng Y, Zhang Q. 1998. Three-dimensional front tracking. *SIAM J. Sci. Comput.* 19 703–27
45. Glimm J, Grove JW, XL Li, Tan DC. 2000. Three-dimensional front tracking. *SIAM J. Sci. Comput.* 21 2240–56
46. Glimm J, Marchesin D, McBryan O. 1981. A numerical-method for 2 phase flow with an unstable interface *J. Comput. Phys.* 39 179–200
47. Glimm J, Xiao LL, Liu Y, Zhao N. 2001. Conservative front tracking and level set algorithms. *Proc. Nat. Acad. Sci.* 98 14198–201
48. Harlow F, Welch J. 1965. Numerical calculation of time-dependent viscous incompressible flow of fluids with free surfaces *Phys. Fluid.* 8 2182-89
49. Harten A, Engquist B, Osher S, Chakravarthy S. 1987a. Uniformly high order accurate essentially non-oscillatory schemes III. *J. Comput. Phys.* 71 231-303.
50. Harten A, Osher SJ. 1987b. Uniformly high order accurate non-oscillatory schemes I.
51. Helmsen J, Puckett EG, Colella P, Dorr M. 1996. Two new methods for simulating photolithography development. *SPIE 1996 International Symposium on Microlithography* SPIE 2726, June.
52. Hou TY, Li ZL, Osher S, Zhao HK. 1997. A hybrid method for moving interface problems with application to the Hele-Shaw flow. *J. Comput. Phys.* 134, 236–52.
53. Kang M, Fedkiw R, Liu LD. 2000. A Boundary Condition Capturing Method for Multiphase Incompressible Flow. *J. Sci. Comput.* 15, 323–60
54. Karma A, Rappel WJ. 1998. Quantitative phase-field modeling of dendritic growth in two and three dimensions. *Phys. Rev. E* 57 4323–49
55. Karni S. 1994. Multi-component flow calculations by a consistent primitive algorithm. *J. Comput. Phys.* 112 31–43
56. Karni S. 1996. Hybrid multifluid algorithms. *SIAM J. Sci. Comput.* 17 1019–39
57. Kim J, Moin P, 1985. Application of a fractional-step method to incompressible Navier-

- Stokes equations. *J. Comput. Phys.* 59 308-323
58. Kim YT, Goldenfeld N, Dantzig J. 2000. Computation of dendritic microstructures using a level set method *Phys. Rev. E* 62 Part B 2471-74
59. Kimmel R, Sethian JA, 1998. Fast Marching Methods on Triangulated Domains *Proc. Nat. Acad. Sci.* 95 8341-843
60. Lafaurie B, Nardone C, Scardovelli R, Zaleski S, Zanetti G. 1994. Modeling merger and fragmentation in multiphase flows with SURFER. *J. Comput. Phys.* 113 134-47
61. LeVeque RJ, Shyu KM. 1996. 2 dimensional front tracking based on high resolution wave propagation methods *SIAM J. Comput. Phys.* 128 354-77
62. Li X, Smereka P, Russo G, Srolovitz DJ. 2002. Simulation of faceted film growth in three-dimensions: microstructure, morphology and texture, in preparation.
63. Lai MF. 1993. A projection method for reacting flow in the zero Mach number limit. PhD thesis, University of California, Berkeley.
64. Liu XD, Fedkiw R, Kang M. 2000. A boundary condition capturing method for Poisson's equation on irregular domains *J. Comput. Phys.* 160 151-78
65. Lowengrub J, Truskinovsky L. 1998. Quasi-incompressible Cahn-Hilliard fluids and topological transitions *P. Roy. Soc. Lond. A Mat.* 454 2617-54
66. Malladi R, Sethian JA, Vemuri BC. 1995. Shape Modeling with Front Propagation: A Level Set Approach *IEEE Trans. on Pattern Analysis and Machine Intelligence* 17 2 158-175
67. Mayo A. 1992. The rapid evaluation of volume integrals of potential theory on general regions. *J. Comp. Phys.* 100 236-45
68. Merriman B, Bence J, Osher SJ. 1994. Motion of Multiple Junctions: A Level Set Approach. *Jour. Comp. Phys.* 112 2 334-363.
69. Mulder W, Osher SJ, Sethian JA. 1992. Computing interfaces in compressible gas dynamics. *J. Comput. Phys.* 100 209-28
70. Osher SJ, Fedkiw RP. 2001. Level set methods: An overview and some recent results. *J. Comput. Phys.* 169 463-502
71. Osher SJ, Merriman B. 1997. The Wulff shape as th asymptotic limit of a growing crystalline interface. *Asian J. Math*, 1, 560.
72. Osher SJ, Sethian JA. 1988. Fronts propagating with curvature dependent speed: algo-

- rithms based on Hamilton-Jacobi formulations. *J. Comput. Phys.* 79 12–49
73. Osher SJ, Shu CW. 1991. High-order essentially nonoscillatory schemes for Hamilton-Jacobi equations *SIAM J. Numer. Anal.* 28 907–22
74. Paritosh, D.J. Srolovitz DJ, Battaile CC, Li X, Butler JE. 1999. Simulation of faceted film growth in two-dimension: microstructure morphology, and texture. *Acta mater.* 47 2269–81
75. Peng DP, Merriman B, Osher S, Zhao HK, Kang MJ. 1999a. A PDE-based fast local level set method. *J. Comp. Phys.* 155 410–38
76. Peng D, Osher SJ, Merriman B, Zhao HK. 1999b. The geometry of Wulff crystal shapes and its relations with Riemann Problems. *Contemp. Math.* 238 251-303, eds. G-Q. Chen and E.D. Benedetto, AMS, Providence.
77. Peskin CS. 1977. Numerical-analysis of blood-flow in heart *J. Comput. Phys.* 25 220–252
78. Puckett EG, Almgren AS, Bell JB, Marcus DL, Rider WJ. 1997. A high-order projection method for tracking fluid interfaces in variable density incompressible flows. *J. Comput. Phys.* 130 269-82
79. Quirk J, Karni S. 1996. On the dynamics of a shock-bubble interaction. *J. Fluid Mech.* 318 129–63
80. Rhee C, Talbot L, Sethian JA. 1995. Dynamical Study of a Premixed V flame. *Jour. Fluid Mech.*, 300, pp. 87–115.
81. Russo G, Smereka P. 2000a. A remark on computing distance functions. *J. Comput Phys.* 163 51–67
82. Russo G, Smereka P. 2000b. A level set method for the evolution of faceted interfaces, *SIAM J. Sci. Comp.* 6 2073-95
83. Russo G, Smereka P. 2002. A narrow band level set method for the computation of polycrystalline thin films, in preparation.
84. Scardovelli R, Zaleski S. 1999. Direct numerical simulation of free-surface and interfacial flow. *Annu. Rev. Fluid Mech.* 31 567–603
85. Sethian JA. 1982. An Analysis of Flame Propagation, Technical Report, Lawrence Berkeley National Laboratory, Dept. of Mathematics, University of California, Berkeley, CA.
86. Sethian JA. 1985. Curvature and the Evolution of Fronts. *Comm. in Math. Phys.* 101

487–499

87. Sethian JA. 1987. Numerical Methods for Propagating Fronts, in Variational Methods for Free Surface Interfaces, Eds. P. Concus and R. Finn, Springer-Verlag, NY.
88. Sethian, JA. 1994. Curvature Flow and Entropy Conditions Applied to Grid Generation. *J. Comp. Phys.* 115 440–454.
89. Sethian JA. 1996a. A Fast Marching Level Set Method for Monotonically Advancing Fronts. *Proc. Nat. Acad. Sci.* 93 4 1591–1595
90. Sethian JA. 1996b. Level Set Methods: Evolving Interfaces in Geometry, Fluid Mechanics, Computer Vision, and Materials Sciences, First Edition, Cambridge University Press
91. Sethian JA. 1996c. A Review of the Theory, Algorithms, and Applications of Level Set Methods for Propagating Interfaces, *Acta Numerica*. Cambridge University Press
92. Sethian JA. 1999a. Level Set Methods and Fast Marching Methods: Evolving Interfaces in Computational Geometry, Fluid Mechanics, Computer Vision and Materials Sciences, Cambridge University Press
93. Sethian JA. 1999b. Fast Marching Methods, *SIAM Review.* 41 2 199-235
94. Sethian JA. 2001. Evolution, Implementation and Application of Level Set and Fast Marching Methods for Advancing Fronts, *Journal Computational Physics* 169 2 503-555
95. Sethian JA, Vladimirsky A. 2001. Ordered Upwind Methods for Static Hamilton-Jacobi Equations. *Proceedings of the National Academy of Sciences* 98 11069-11074
96. Sethian JA, Yu JD. 2002. A Second-order Projection Method For Two-dimensional/Axi-Symmetric Two-Fluid Flows. *Center for Pure and Applied Mathematics, Report*, Univ. of California, Berkeley, in progress
97. Shu CW, Osher SJ. 1988. Efficient implementation of essentially non-oscillatory shock capturing schemes. *J. Comput Phys.* 77 439–71
98. Shu CW, Osher SJ. 1989. Efficient implementation of essentially non-oscillatory shock capturing schemes II. *J. Comput Phys.* 83 32–78
99. Smereka P. 1996. Level set methods for two-fluid flows. Lectures notes from INRIA short course. available at www.math.lsa.umich.edu/~psmereka
100. Smereka P. 2000. Spiral Crystal Growth, *Physica D* 138 282–301
101. Smereka P. 2003. Semi-implicit level set methods for flows by mean curvature and surface

- diffusion *J. Sci. Comp.* (to appear).
102. Smith KA, Solis FJ, Chopp DL. 2001. A projection method for motion of triple junctions by level sets. *Interfaces and Free Boundaries, 2001*) to appear.
 103. Son G, Dhir VK. 1998. Numerical simulation of film boiling near critical pressures with a level set method. *J. Heat Trans. T. ASME* 120 183–92.
 104. Soravia P. 1994. Generalized motion of a front propagating along its normal direction: a differential games approach. *Nonlinear Anal., Theory, Meth. Appl.* 22 1247–62
 105. Strain J. 1999. Semi-Lagrangian Methods for Level Set Equations *J. Comput. Phys.* 151 498-533.
 106. Strain J. 1999. Tree Methods for Moving Interfaces *J. Comput. Phys.* 151 616-648.
 107. Strain J. 1999. Fast Tree-based Redistancing for Level Set Computations *J. Comput. Phys.* 152 648-666.
 108. Sukumar N, Chopp DL, Moes N, Belytschko T. 2001. Modeling holes and inclusions by level sets in the extended finite-element method *Comput. Method Appl. M.* 190 6183–200
 109. Sussman M. 2001. An adaptive mesh algorithm for free surface flows in general geometries. in *Adaptive Method of lines*, CRC press.
 110. Sussman M. 2002a. Personal communication.
 111. Sussman M. 2002b. A second order coupled level set and volume-of-fluid method for computing growth and collapse of vapor bubbles, submitted for publication.
 112. Sussman M, Almgren AS, Bell JB, Colella P, Howell L, Welcome M. 1999. An adaptive level set approach for incompressible two-phase flows. *J. Comput. Phys.* 148 81-124
 113. Sussman M, Dommermuth DG. 2000. The numerical simulation of ship waves using Cartesian grid methods. In Proceedings of the Twenty Third Symposium on Naval Hydrodynamics, Val-De-Reuil, France, September 2000.
 114. Sussman M, Fatemi E. 1999. An efficient interface preserving level set re-distancing algorithm and its application to interfacial incompressible fluid flow. *SIAM J. Sci. Comput.* 20 1165–91
 115. Sussman M, Fatemi E, Smereka P, Osher S. 1998. An improved level set method of incompressible two-fluid flows. *Comput. Fluids* 27 663–80
 116. Sussman M, Puckett EG. 2000. A coupled level set and volume-of-fluid method for comput-

- ing 3D and axisymmetric incompressible two-phase flows. *J. Comput. Phys.* 162 301–37
117. Sussman M, Smereka P. 1997. Axisymmetric free boundary problems. *J. Fluid Mech.* 341 269–94
118. Sussman M, Smereka P, Osher SJ. 1994. A level set approach to computing solutions to incompressible two-phase flow. *J. Comput. Phys.* 114 146–159.
119. Taylor JE, Cahn J, Handwerker CA. 1992. Geometrical models of crystal growth *Acta Metall. Mater.* 40 1443–74
120. Trebotich DP, Colella P. 2001. A Projection Method for Incompressible Viscous Flow on Moving Quadrilateral Grid. *J. Comput. Phys.*, 166, pp. 191-217.
121. Tryggvason G, Bunner B, Esmaeeli A, Juric D, Al-Rawahi N, Tauber W, Han J, Nas S, Jan YJ. 2001. A front-tracking method for the computations of multiphase flow *J. Comput. Phys.*, 169, 708–59.
122. Tsitsiklis JN. 1995. Efficient Algorithms for Globally Optimal Trajectories, *IEEE Transactions on Automatic Control* 40 1528-1538
123. Unverdi SO, Tryggvason G. 1992. A front-tracking method for viscous, incompressible, multi-fluid flows. *J. Comput. Phys.* 100 25–37
124. van der Drift A. 1967. Evolutionary selection, a principle governing growth orientation in vapor-deposited layers *Philips Res. Repts.* 22 267–88
125. Wheeler AA, Murray BT, Schaefer RJ. 1993. Computation of Dendrites using a phase field model. *Physica D* 66 243–62.
126. Wulff G. 1901 Frage der Geschwindigkeit des Wachstums und der Anflosung der Kristallflächen, *Z. Krystall. Min* 34 449-530
127. Zhao, HK, Chan T, Merriman B, Osher SJ, 1996, A variational level set approach to multiphase motion, *J. Comput. Phys.* 127 179–95
128. Zhao, HK, Merriman B, Osher SJ, Wang L. 1998. Capturing the behavior of bubbles and drops using the variational level set approach *J. Comput. Phys.* 127 495–518
129. Zhu J, Ronney PD. 1995. Simulation of Front Propagation at Large Non-dimensional Flow Disturbance Intensities *Comb. Sci. Tech.* 100 183–201
130. Zhu, J, Sethian, JA, 1992. Projection Methods Coupled to Level Set Interface Techniques *J. Comp. Phys.* 102 128–138

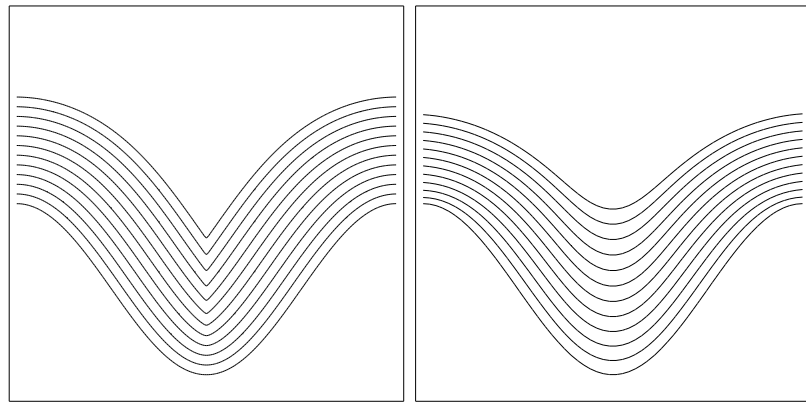
Fig. 1(a) $F = 1$ Fig. 1(b) $F = 1 - 0.25\kappa$

Figure 1: Entropy solution is the limit of viscous solutions.

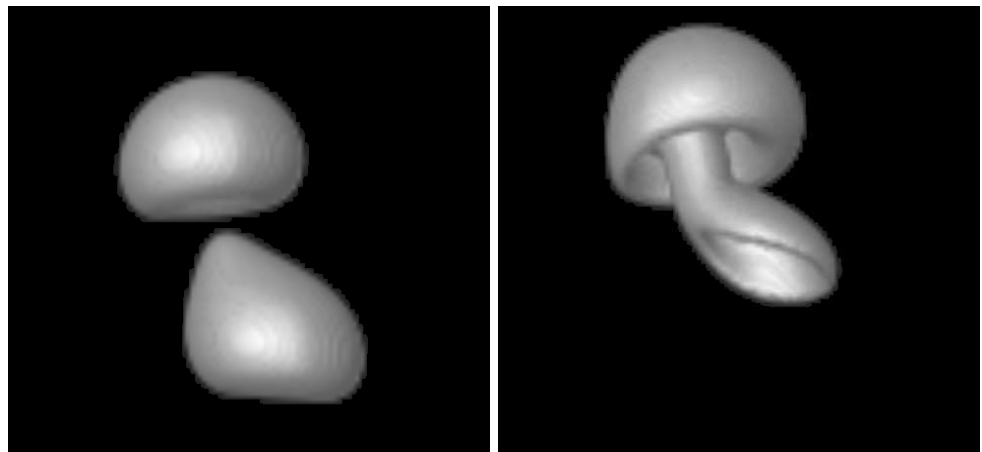


Figure 2: Evolution of two bubbles from Sussman & Puckett (2000)

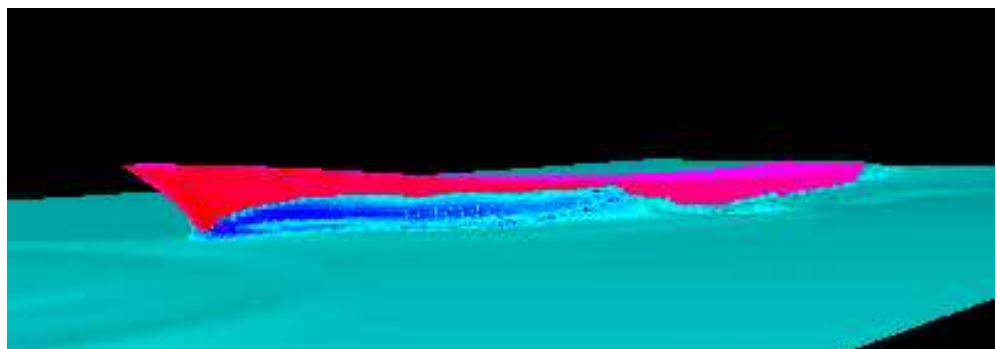


Figure 3: Computation of a ship wake from Sussman & Dommermuth (2000)

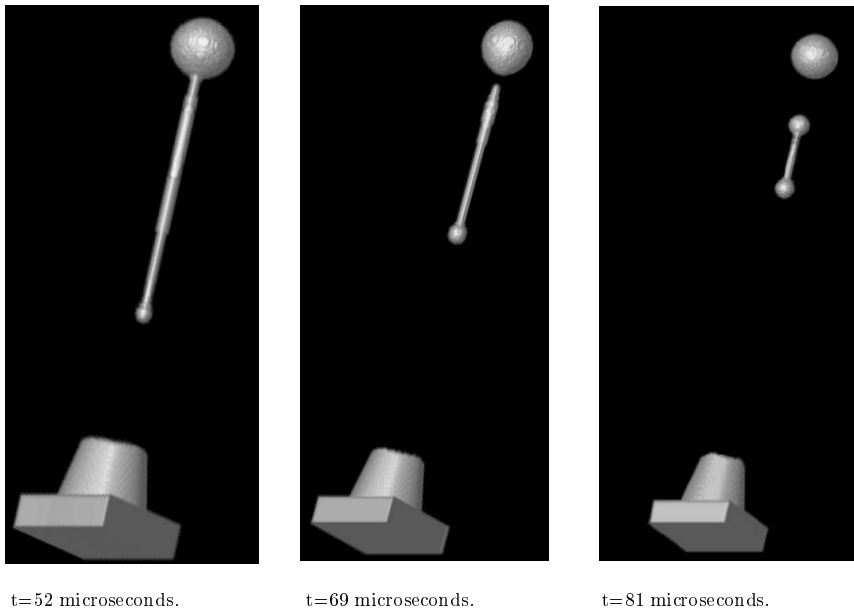


Figure 4: Evolution an inkjet from Aleinov et al (1999)

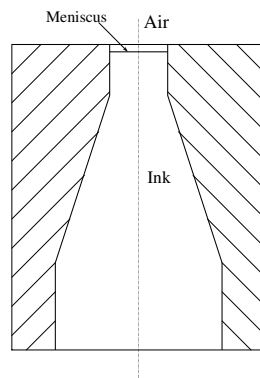


Figure 5: The cross section view of an inkjet nozzle.

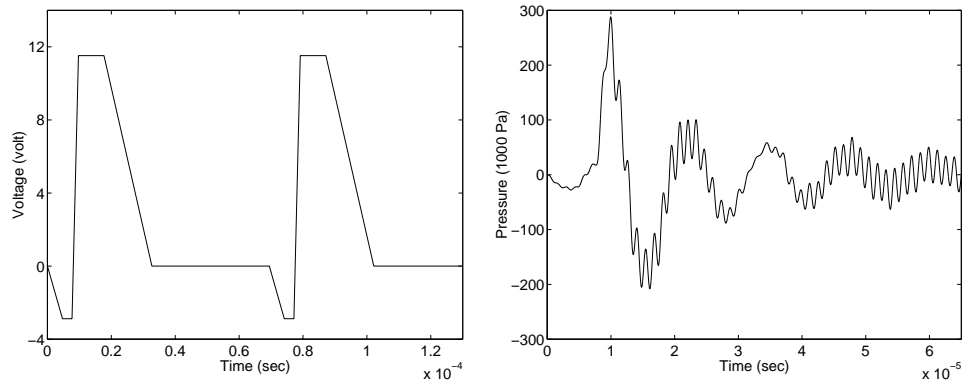


Fig. 6a; Inkjet driving voltage

6b: Inflow pressure

Figure 6: Electric Circuit Model

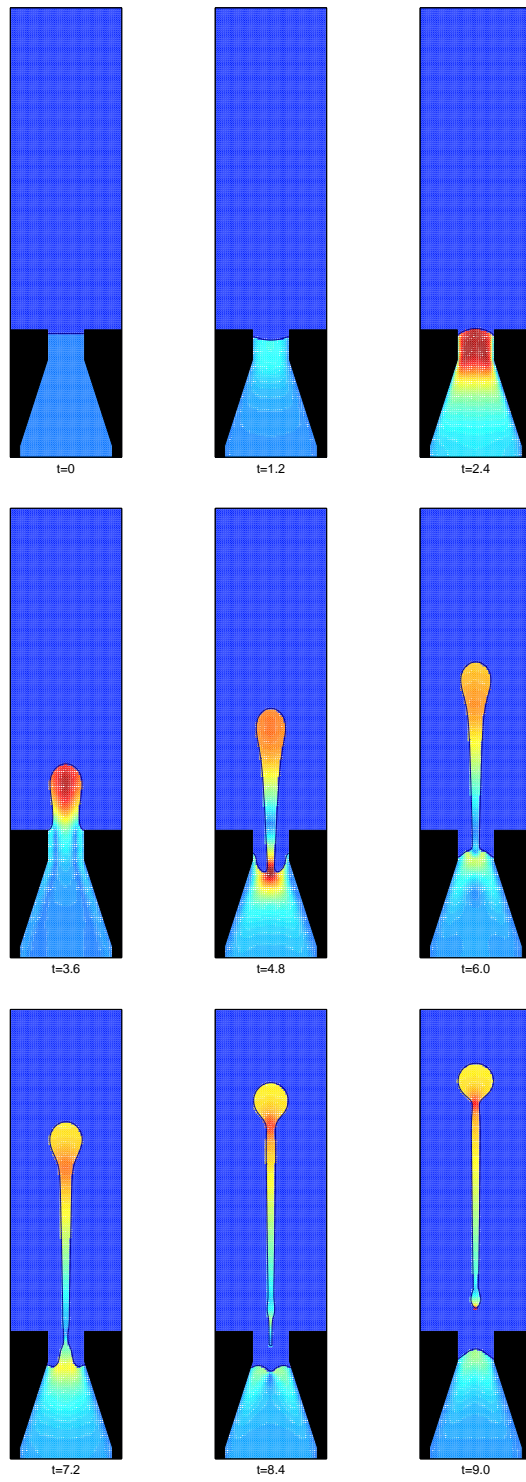


Figure 7: Ejection of an ink droplet.

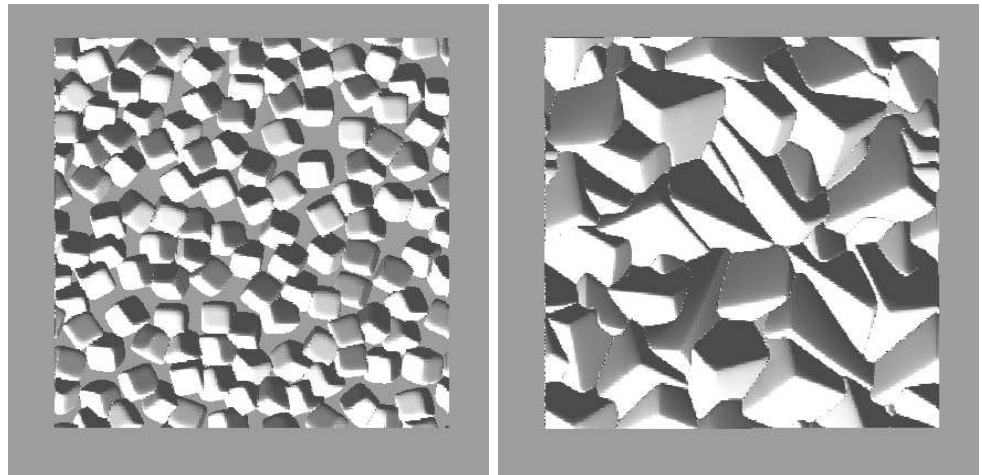


Figure 8: The growth of a diamond film. Here the diamond grows with a cubic structure. The figure on the left is at an early time whereas the figure on the right is at a later time. From Li et al (2002).

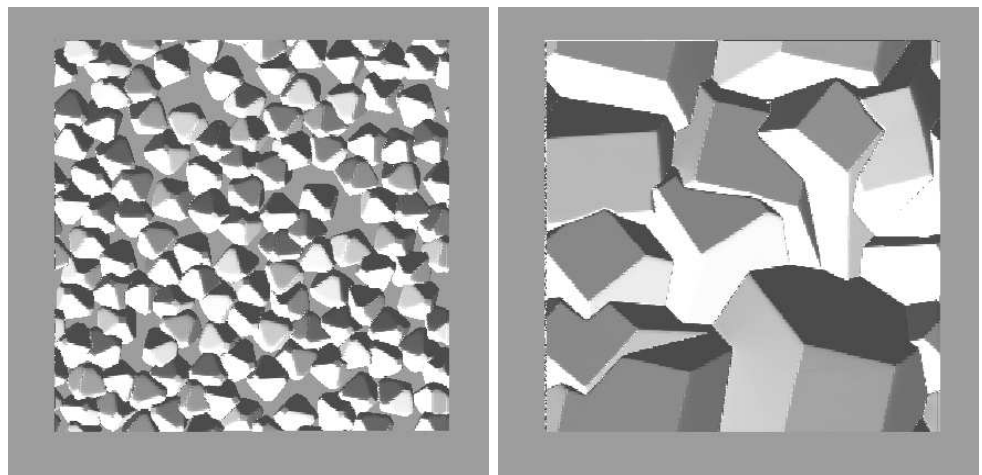


Figure 9: The growth of a diamond film. Here the diamond grows as a 14-sided polyhedron. The figure on the left is at an early time whereas the figure on the right is at a later time. From Li et al (2002).